Sensitivities of prospective future e^+e^- colliders to decoupled new physics

John Ellis[a,b] **and Tevong You**[a,c,d]

[a] *Theoretical Particle Physics and Cosmology Group,*
  Physics Department, King's College London,
  London WC2R 2LS, U.K.

[b] *TH Division, Physics Department, CERN,*
  CH-1211 Geneva 23, Switzerland

[c] *Cavendish Laboratory, University of Cambridge,*
  J.J. Thomson Avenue, Cambridge, CB3 0HE, U.K.

[d] *DAMTP, University of Cambridge,*
  Wilberforce Road, Cambridge, CB3 0WA, U.K.

  E-mail: john.ellis@cern.ch, tty20@cam.ac.uk

ABSTRACT: We explore the indirect sensitivities to decoupled new physics of prospective precision electroweak measurements, triple-gauge-coupling measurements and Higgs physics at future e^+e^- colliders, with emphasis on the ILC250 and FCC-ee. The Standard Model effective field theory (SM EFT) is adopted as a model-independent approach for relating experimental precision projections to the scale of new physics, and we present prospective constraints on the Wilson coefficients of dimension-6 operators. We find that in a marginalised fit ILC250 EWPT measurements may be sensitive to new physics scales $\Lambda = \mathcal{O}(10)\,\mathrm{TeV}$, and FCC-ee EWPT measurements may be sensitive to $\Lambda = \mathcal{O}(30)\,\mathrm{TeV}$. The prospective sensitivities of Higgs and TGC measurements at the ILC250 (FCC-ee) are to $\Lambda = \mathcal{O}(1)\,\mathrm{TeV}$ ($\Lambda = \mathcal{O}(2)\,\mathrm{TeV}$).

JHEP03(2016)089

Contents

1 Introduction

At the time of writing, all measurements of the known particles persist in remaining consistent with their properties as predicted in the Standard Model (SM), and there are no convincing signals at the LHC of any particles beyond those in the SM. In particular, the couplings of the Higgs boson [1, 2] have recently been analysed using the combined ATLAS and CMS data, with no signs of new physics [3]. Under these circumstances, it is natural to assume that it is 'the' SM Higgs boson, and suppose that any new physics must involve massive particles that are decoupled from physics at the energies explored so far [4]. A powerful tool for analysing such models of physics beyond the SM is provided by the SM Effective Field Theory (SM EFT), which parametrises possible new physics via a systematic expansion in a series of higher-dimensional operators composed of SM fields [5, 6]. The most important rôle in this approach is played by operators of dimension 6,[1] whose matching to ultraviolet (UV) models is greatly simplified by the universal one-loop effective action when such operators are loop-induced [10–12].

The SM EFT has already been used in several analyses [13–32] of the available data from the LHC and previous accelerators including LEP and the SLC, which set the standard for electroweak precision tests (EWPTs).[2] As reviewed in section 2 of this paper, there are certain (combinations of) dimension-6 operators whose coefficients are particularly tightly constrained by these EWPTs. On the other hand, the coefficients of other (combinations of) operators are constrained by other measurements, including Higgs physics and triple-gauge

---

[1]The unique dimension-5 operator is the well-known Weinberg neutrino-mass operator [7]. See refs. [8] and [9] for a classification of dimension-7 and -8 operators.

[2]Different operator bases in the literature may be translated between each other using the `Rosetta` tool [33].

couplings (TGCs). Together with Verónica Sanz, we have previously published a global analysis of dimension-6 operators in the SM EFT [22, 23], providing 95% CL ranges for their coefficients, both when each operator is switched on individually and when marginalising over the possible coefficients of all contributing operators.[3]

There is currently growing interest in the physics accessible to possible future e^+e^- colliders that would continue the studies made with LEP and the SLC to higher energies and or luminosities [34–44]. One of the primary objectives of such machines will be make detailed studies of the Higgs boson and its interactions, with other possible elements of their physics programmes including studies at the Z peak with very high luminosities, studies of W^+W^- production close to threshold and above, measurements near the $\bar{t}t$ threshold and, of course, searches for possible new particles.

In this paper we explore the implications within the SM EFT of the high-precision physics possible with relatively low-energy e^+e^- colliders, considering in particular the ILC running at $250\,\mathrm{GeV}$ with an integrated luminosity of $250\,\mathrm{fb}^{-1}$ [36–38], the scenario we call ILC250, and FCC-ee with $10\,\mathrm{ab}^{-1}$ at a centre-of mass energy of $240\,\mathrm{GeV}$ [40], both accompanied by lower-energy running at the Z peak and the W^+W^- threshold. We do not consider the possibilities for producing directly new particles, which are relatively limited at these centre-of-mass energies.

In section 2 of this paper we review briefly relevant aspects of the SM EFT, identifying the operators of dimension 6 that are most relevant for the observables we consider. We then consider in section 3 the formalism we use for analysing prospective measurements of electroweak precision measurements, exhibiting the corrections to SM predictions for EWPTs that one finds at first order in the SM EFT coefficients. This is followed by analyses of the prospective constraints on these coefficients that could be provided by ILC250 and FCC-ee measurements. We then present a corresponding discussion of possible contributions within the SM EFT to Higgs physics and TGC measurements, as well as analyses of the sensitivities to the corresponding of ILC250 and FCC-ee. As we discuss, the prospective constraints on some (combinations of) operator coefficients are so tight that they may as well be set to zero in the analyses of Higgs physics and TGCs.

When translated into the effective mass scales Λ to which the prospective measurements are able to reach, we find that ILC250 EWPT measurements could be sensitive to $\Lambda = \mathcal{O}(10)\,\mathrm{TeV}$, and FCC-ee EWPT measurements could be sensitive to $\Lambda = \mathcal{O}(30)\,\mathrm{TeV}$, when marginalised over the effects of all relevant dimension-6 operators. The corresponding sensitivities of Higgs and TGC measurements at the ILC250 (FCC-ee) are to $\Lambda = \mathcal{O}(1)\,\mathrm{TeV}$ ($\Lambda = \mathcal{O}(2)\,\mathrm{TeV}$).

2 The Standard Model Effective Field Theory

In the Standard Model Effective Field Theory (SM EFT) the renormalisable interactions in the SM are supplemented by higher-dimensional operators. These are composed of all possible combinations of SM fields that respect the $\mathrm{SU}(3)_c \times \mathrm{SU}(2)_L \times \mathrm{U}(1)_Y$ gauge symmetries and Lorentz invariance, with the leading lepton-number-conserving effects parametrised by

---

[3]For other similar global fits to dimension-6 operators, see for example, refs. [17, 18, 21, 29].

EWPTs	Higgs Physics	TGCs
$\mathcal{O}_W = \frac{ig}{2}\left(H^\dagger \sigma^a \overset{\leftrightarrow}{D^\mu} H\right) D^\nu W^a_{\mu\nu}$		
$\mathcal{O}_B = \frac{ig'}{2}\left(H^\dagger \overset{\leftrightarrow}{D^\mu} H\right) \partial^\nu B_{\mu\nu}$		$\mathcal{O}_{3W} = g\frac{\epsilon_{abc}}{3!} W^{a\,\nu}_\mu W^b_{\nu\rho} W^{c\,\rho\mu}$
$\mathcal{O}_T = \frac{1}{2}\left(H^\dagger \overset{\leftrightarrow}{D}_\mu H\right)^2$	$\mathcal{O}_{HW} = ig(D^\mu H)^\dagger \sigma^a (D^\nu H) W^a_{\mu\nu}$	
$\mathcal{O}^{(3)\,l}_{LL} = (\bar{L}_L \sigma^a \gamma^\mu L_L)(\bar{L}_L \sigma^a \gamma_\mu L_L)$	$\mathcal{O}_{HB} = ig'(D^\mu H)^\dagger (D^\nu H) B_{\mu\nu}$	
$\mathcal{O}^e_R = (iH^\dagger \overset{\leftrightarrow}{D}_\mu H)(\bar{e}_R \gamma^\mu e_R)$	$\mathcal{O}_g = g_s^2 |H|^2 G^A_{\mu\nu} G^{A\mu\nu}$	
$\mathcal{O}^u_R = (iH^\dagger \overset{\leftrightarrow}{D}_\mu H)(\bar{u}_R \gamma^\mu u_R)$	$\mathcal{O}_\gamma = g'^2 |H|^2 B_{\mu\nu} B^{\mu\nu}$	
$\mathcal{O}^d_R = (iH^\dagger \overset{\leftrightarrow}{D}_\mu H)(\bar{d}_R \gamma^\mu d_R)$	$\mathcal{O}_H = \frac{1}{2}(\partial^\mu |H|^2)^2$	
$\mathcal{O}^{(3)\,q}_L = (iH^\dagger \sigma^a \overset{\leftrightarrow}{D}_\mu H)(\bar{Q}_L \sigma^a \gamma^\mu Q_L)$	$\mathcal{O}_f = y_f |H|^2 \bar{F}_L H^{(c)} f_R + \text{h.c.}$	
$\mathcal{O}^q_L = (iH^\dagger \overset{\leftrightarrow}{D}_\mu H)(\bar{Q}_L \gamma^\mu Q_L)$	$\mathcal{O}_6 = \lambda |H|^6$	

Table 1. List of CP-even dimension-6 operators in our chosen basis [21], noting in each case the categories of observables that place the strongest constraints on the operator or its linear combinations with other operators.

dimension $d \geq 6$ operators with unknown Wilson coefficients that could be generated by decoupled new physics beyond the SM, assuming that these also respect the SM gauge symmetries. According to the decoupling assumption, the effects of operators with dimensions $d > 6$ are sub-leading, so we consider just the dimension-6 SM EFT Lagrangian

$$\mathcal{L}_{\text{SMEFT}} = \mathcal{L}_{\text{SM}} + \sum_i \frac{c_i}{\Lambda^2} \mathcal{O}_i \,, \tag{2.1}$$

where the $\mathcal{O}_i$ are the dimension-6 operators in the basis of ref. [21] that we adopt here, Λ represents the scale of new physics, and the coefficients c_i depend on the details of its structure. The operators relevant for the observables included in our fits are listed in table 1, where we assume CP conservation and a flavour-blind structure for the operators involving SM fermions.[4]

The high-sensitivity electroweak precision tests (EWPTs), particularly those using the leptonic subset of Z-pole observables, impose the strongest constraints on the following dimension-6 operators:

$$\mathcal{L}^{\text{EWPT}}_{\text{dim-6}} \supset \frac{1}{2}\frac{(\bar{c}_W + \bar{c}_B)}{m_W^2}(\mathcal{O}_W + \mathcal{O}_B) + \frac{\bar{c}_T}{v^2}\mathcal{O}_T + \frac{\bar{c}^{(3)l}_{LL}}{v^2}\mathcal{O}^{(3)l}_{LL} + \frac{\bar{c}^e_R}{v^2}\mathcal{O}^e_R \,, \tag{2.2}$$

where we introduce coefficients $\bar{c}_i$ whose normalisations differ from those in (2.1) by squared ratios of the electroweak scale to the nominal new-physics scale Λ:

$$\bar{c}_i = c_i \frac{M^2}{\Lambda^2} \,, \tag{2.3}$$

where $M \equiv v, m_W$ depending on the operator.

---

[4]For studies that relax some of the flavour assumptions, see for example refs. [27, 30].

On the other hand, the dimension-6 operators and their linear combinations that affect Higgs physics and measurements of triple-gauge couplings (TGCs) in our fits are given by

$$\mathcal{L}_{\text{dim-6}}^{\text{Higgs+TGC}} \supset \frac{1}{2} \frac{(\bar{c}_W - \bar{c}_B)}{m_W^2} (\mathcal{O}_W - \mathcal{O}_B) + \frac{\bar{c}_{HW}}{m_W^2} \mathcal{O}_{HW} + \frac{\bar{c}_{HB}}{m_W^2} \mathcal{O}_{HB} + \frac{\bar{c}_g}{m_W^2} \mathcal{O}_g + \frac{\bar{c}_\gamma}{m_W^2} \mathcal{O}_\gamma$$

$$+ \frac{\bar{c}_H}{v^2} \mathcal{O}_H + \frac{\bar{c}_f}{v^2} \mathcal{O}_f \,. \tag{2.4}$$

Since the linear combination $\bar{c}_W + \bar{c}_B$ is potentially constrained very strongly by EWPTs, we set $\bar{c}_B = -\bar{c}_W$ in the fits to Higgs physics and the TGCs.

We note that the coefficients constrained in our fit correspond to those defined at the electroweak scale, $c_i \equiv c_i(v)$, which can be related to $c_i(\Lambda)$ at the matching scale by RGE running [45–52]. We neglect dimension-8 operators in our analysis, as well as four-fermion operators (other than $\bar{c}_{LL}^{(3)l}$ that modifies the input parameter G_F), whose effects on Z-pole measurements are formally of the same order as dimension-8 operators due to the lack of linear interference terms with the SM amplitudes [16]. The effects of these operators and other omitted theory uncertainties may be important for $\Lambda \lesssim 3\,\text{TeV}$ [25, 26] but, as we will see in the next section, the UV cut-off scale for future electroweak precision measurements can be assumed to be beyond this.

3   Electroweak Precision Tests

We use in our analyses of the electroweak precision tests (EWPTs) the W mass and the following Z-peak pseudo-observables:

$$\Gamma_Z = \Gamma_{\text{had}} + 3\Gamma_l + 3\Gamma_\nu \,, \qquad R_l = \frac{\Gamma_{\text{had}}}{\Gamma_l} \,, \qquad R_q = \frac{\Gamma_q}{\Gamma_{\text{had}}} \,,$$

$$\sigma_{\text{had}} = 12\pi \frac{\Gamma_e \Gamma_{\text{had}}}{\hat{m}_Z^2 \Gamma_Z^2} \,, \qquad A_{FB}^f = \frac{3}{4} A_e A_f \,, \qquad m_W = c_W m_Z \,.$$

These are functions of the decay widths and asymmetries:

$$\Gamma_f = \frac{\sqrt{2} G_F m_Z^2 \hat{m}_Z}{6\pi} \left(g_{f_L}^2 + g_{f_R}^2 \right) \,,$$

$$A_f = \frac{g_{f_L}^2 - g_{f_R}^2}{g_{f_L}^2 + g_{f_R}^2} \,,$$

which depend in turn upon modifications to the $Z\bar{f}f$ couplings:

$$g_{f_L} = g_{f_L}^{\text{SM}} + \delta g_{f_L} \,, \quad g_{f_R} = g_{f_R}^{\text{SM}} + \delta g_{f_R} \,,$$

where $g_f^{\text{SM}} = T_f^3 - Q_f s_W^2$. These observables receive direct contributions from $\bar{c}_R^e, \bar{c}_R^u, \bar{c}_R^d, \bar{c}_L^q$ and $\bar{c}_L^{(3)q}$ through the following coupling modifications:[5]

$$\xi_{g_R^l} \supset -\frac{1}{2} \frac{c_R^l}{g_R^l} \,, \qquad \xi_{g_L^l} \supset 0 \,, \tag{3.1}$$

$$\xi_{g_R^q} \supset -\frac{1}{2} \frac{c_R^q}{g_R^q} \,, \qquad \xi_{g_L^q} \supset \frac{T_q^3 c_L^{(3)q} - \frac{1}{2} c_L^q}{g_L^q} \,, \tag{3.2}$$

---

[5]They also depend on the coefficients $\bar{c}_L^L$ and $\bar{c}_L^{(3)L}$ of operators that are eliminated in the basis we use [21].

where we have defined the fractional shifts $\xi_X \equiv \delta X/X$, and we use the symbol $\supset$ to indicate that there are further shifts from other dimension-6 operators. The decay widths and asymmetries are then modified as follows:

$$\xi_{\Gamma_f} \supset 2\frac{g_{f_L}^2 \xi_{g_{f_L}} + g_{f_R}^2 \xi_{g_{f_R}}}{g_{f_L}^2 + g_{f_R}^2}\,, \qquad \xi_{A_f} = 4\frac{g_{f_L}^2 g_{f_R}^2}{g_{f_L}^4 - g_{f_R}^4}\left(\xi_{g_{f_L}} - \xi_{g_{f_R}}\right)\,.$$

There are also indirect corrections from the four-fermion operator $\bar{c}_{LL}^{(3)l}$, which modifies the input observable G_F so that

$$\xi_{\Gamma_f} \supset \xi_{G_F}\,, \qquad \xi_{g_{L,R}^f} \supset \frac{-Q_f s_W^2}{T_f^3 - Q_f s_W^2}\xi_{s_W^2}\,, \qquad \xi_{m_W} \supset -\frac{1}{2}\frac{s_W^2}{c_W^2}\xi_{s_W^2}\,.$$

Since $s_W^2 = \frac{1}{2} - \frac{1}{2}\sqrt{1 - \frac{4\pi\alpha}{\sqrt{2}G_F m_Z^2}}$, there is a dependence of the weak mixing angle θ_W on the modifications to G_F:

$$\xi_{s_W^2} \supset -\frac{c_W^2}{c_{2W}}\xi_{G_F}\,.$$

Finally, there are also indirect corrections from the oblique corrections $\hat{S} \equiv \bar{c}_W + \bar{c}_B$ and $\hat{T} \equiv \bar{c}_T$ arising from contributions to self-energies $\delta\pi_{VV}$:

$$\delta\pi_{ZZ} = -\hat{T} + 2\hat{S}s_W^2\,, \qquad \delta\pi'_{ZZ} = 2\hat{S}s_W^2\,,$$
$$\delta\pi_{\gamma Z} = -\hat{S}c_{2W}t_W\,, \qquad \delta'\gamma\gamma = -2\hat{S}s_W^2\,,$$

where the self-energies π_{VV} are defined as

$$\pi_{ZZ} \equiv \frac{\pi_{ZZ}(m_Z^2)}{m_Z^2}\,, \qquad \pi'_{ZZ} \equiv \lim_{q^2 \to m_Z^2}\frac{\pi_{ZZ}(q^2) - \pi_{ZZ}(m_Z^2)}{q^2 - m_Z^2}\,,$$
$$\pi_{\gamma Z} \equiv \frac{\pi_{\gamma Z}(m_Z^2)}{m_Z^2}\,, \qquad \pi'_{\gamma\gamma} \equiv \lim_{q^2 \to 0}\frac{\pi_{\gamma\gamma}(q^2) - \pi_{\gamma\gamma}(0)}{q^2}\,,$$
$$\pi_{WW} \equiv \frac{\pi_{WW}(m_W^2)}{m_W^2}\,, \qquad \pi_{WW}^0 \equiv \frac{\pi_{WW}(0)}{m_W^2}\,.$$

These modifications affect the EWPTs through the corrections

$$m_Z^2 = (m_Z^2)^0(1 + \pi_{ZZ})\,, \qquad G_F = G_F^0(1 - \pi_{WW}^0)\,, \qquad \alpha(m_Z) = \alpha^0(m_Z)(1 + \pi'_{\gamma\gamma})\,,$$
$$m_W^2 = (m_W^2)^0(1 + \pi_{WW})\,, \qquad \sin^2\theta_{\text{eff}}^f = s_W^2\left(1 - \frac{c_W}{s_W}\pi_{\gamma Z}\right)\,.$$

Using these results and the definition of s_W^2 gives

$$\xi_{s_W^2} = \frac{c_W^2}{c_{2W}}\left(-\delta\pi'_{\gamma\gamma} + \delta\pi_{ZZ} - \delta\pi_{WW}^0 - \frac{c_{2W}}{s_W c_W}\delta\pi_{\gamma Z}\right)\,.$$

Similarly, including all the previously-calculated corrections, we find for the decay width and W mass that

$$\xi_{\Gamma_f} = \delta\pi'_{ZZ} - \delta\pi_{ZZ} + \xi_{G_F}\,,$$
$$\xi_{m_W} = -\frac{1}{2}\frac{s_W^2}{c_W^2}\xi_{s_W^2} + \frac{1}{2}\delta\pi_{ZZ} + \frac{1}{2}\delta\pi_{WW}\,.$$

Focusing on the leptonic subset of observables, we may summarise numerically the dependences of the observables on the dimension-6 operator coefficients using the above tree-level expressions for the observables as follows:

$$\xi_{\Gamma_Z} = -2.69\bar{c}_{LL}^{(3)l} - 0.19\bar{c}_R^e + 1.35\bar{c}_T - 0.90\bar{c}_V^+ ,$$
$$\xi_{\sigma_{\text{had}}^0} = 0.054\bar{c}_{LL}^{(3)l} - 1.46\bar{c}_R^e - 0.03\bar{c}_T + 0.07\bar{c}_V^+ ,$$
$$\xi_{R_e} = -0.56\bar{c}_{LL}^{(3)l} + 1.84\bar{c}_R^e + 0.28\bar{c}_T - 0.73\bar{c}_V^+ ,$$
$$\xi_{A_{FB}^e} = -71.38\bar{c}_{LL}^{(3)l} + 28.89\bar{c}_R^e + 35.69\bar{c}_T - 92.90\bar{c}_V^+ ,$$
$$\xi_{m_W} = -0.43\bar{c}_{LL}^{(3)l} + 0.72\bar{c}_T - 1.02\bar{c}_V^+ ,$$
$$\xi_{A_e} = -35.70\bar{c}_{LL}^{(3)l} + 14.44\bar{c}_R^e + 17.84\bar{c}_T - 46.45\bar{c}_V^+ . \tag{3.3}$$

Here we have used $s_W^2|^{\text{SM}} \equiv 0.23162$, corresponding to the value obtained when relating the EWPT observables to the input parameters for the SM alone, to the highest theoretical precision available [53].

However, since we are neglecting the one-loop contributions from dimension-6 operators this precision is formally of a higher order in the calculations of the expansion coefficients, and we may equally well use $s_W^2|^{\text{tree}} \equiv 0.21221$, which is the value obtained using the tree-level expressions to relate the EWPT observables to the input parameters [24]. Varying s_W^2 between these values can therefore give an indication of the importance of these higher-order effects and is responsible, for example, for the differences between the current EWPT limits given in [22, 23] and in [21]. Including consistently the effects of dimension-6 operators at the loop level would require going beyond the tree level when calculating the expansion coefficients in (3.3). The importance of this omission can also be estimated by calculating numerically the parametric dependences of observables using ZFITTER [54], as in [53], which includes the higher-loop contributions of input parameter modifications in the SM but still neglects the full loop contributions of the dimension-6 operators.[6] A complete study including the effects of dimension-6 operators at loop level is beyond the scope of this note.

3.1 EWPT constraints from the ILC

We take the following 1-σ ILC experimental errors for the observables $\{m_W, \Gamma_Z, R_l, A_e\}$ from [35]:

$$\sigma_{m_W} = 0.005\,\text{GeV} , \qquad \sigma_{\Gamma_Z} = 0.001\,\text{GeV} , \qquad \sigma_{R_l} = 0.01 , \qquad \sigma_{A_e} = 0.0001 . \tag{3.4}$$

We neglect theoretical uncertainties in the SM predictions for these quantities for the purposes of our analysis. For reference, we recall that the current theoretical uncertainty in the SM prediction of m_W is estimated to be $4\,\text{MeV}$, which is potentially reducible to $\sim 1\,\text{MeV}$ when higher-order contributions are calculated in the future [35]. We assume that this will occur within the time-scale of the measurements considered here.

The result of a χ^2 fit to the prospective ILC EWPT measurements assuming Gaussian errors, switching on each operator individually and setting the others to zero, is shown in

---

[6]For some studies of including dimension-6 operators at the loop level see, for example, refs. [55–57].
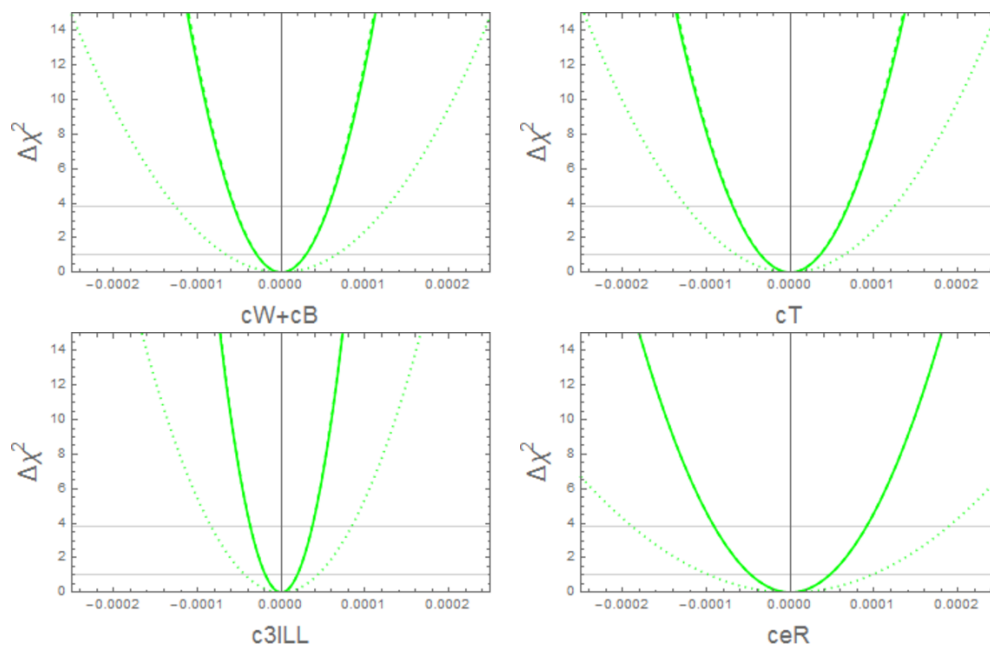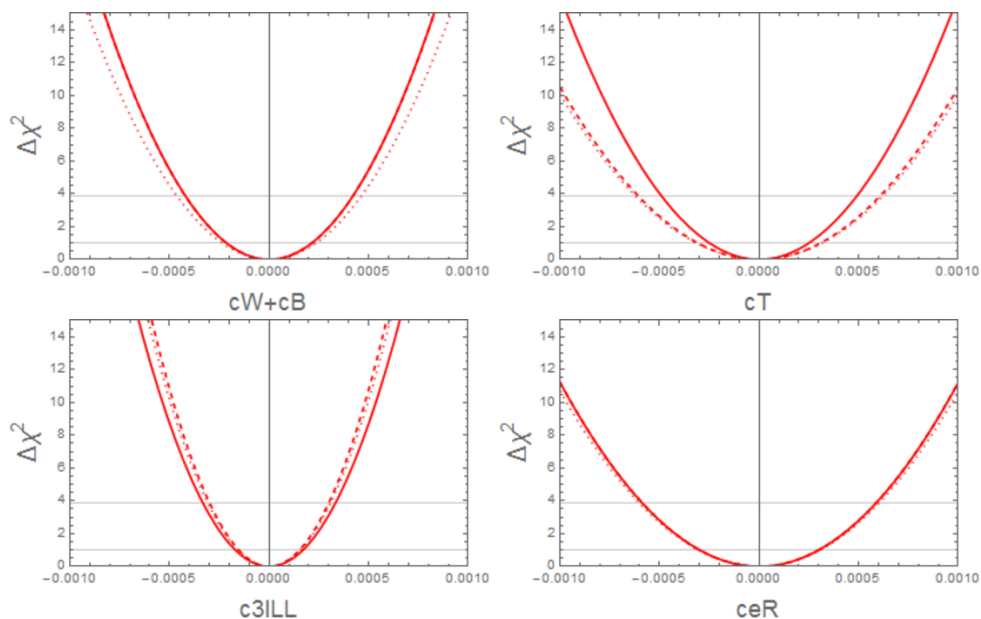
Figure 1. Prospective constraints on individual operator coefficients from ILC EWPT measurements. The projected $\Delta\chi^2$ for each operator affecting the leptonic subset of EWPT observables when switched on one at a time with the others set to zero, incorporating the prospective ILC measurements [35]. The solid (dotted) lines are for dimension-6 contributions computed using the tree-level expressions with $s_W^2|^{\text{SM}}$ ($s_W^2|^{\text{tree}}$), whereas the dashed lines (indistinguishable here from the solid lines) are computed numerically using ZFITTER in the expansion framework of [53].

figure 1. The solid and dotted lines denote the dimension-6 contributions to the EWPT observables using the tree-level expressions with $s_W^2|^{\text{SM}}$ and $s_W^2|^{\text{tree}}$ respectively. The dashed line represents the result of using ZFITTER in the expansion formalism of [53] to calculate the dimension-6 contributions including the higher-order corrections to the parametric dependences. In this case we see results that are practically identical to the solid lines, with 95% CL limits at the $\sim 10^{-5}$ level.

The marginalised χ^2 for a fit allowing all four dimension-6 operators to vary simultaneously is displayed in figure 2, where we see that the limits extend to $\sim 10^{-4}$. In this case some small differences can be observed between the solid and dashed lines for $\bar{c}_R^e$ and $\bar{c}_{LL}^{(3)l}$, whereas none are visible for $\bar{c}_R^e$ and $\bar{c}_W + \bar{c}_B$. In the case of $\bar{c}_R^e$, this is due to the fact that both calculations use $s_W^2|^{\text{SM}}$, and at tree level $\bar{c}_R^e$ does not modify the input parameters whose higher-order contributions are taken into account in the dashed lines, so that no difference is expected.

The projected individual and marginalised 95% CL ILC uncertainties in the four dimension-6 operators are shown in green and red respectively in figure 3. The upper axis converts the limits on the barred coefficients $\bar{c}_i$ to an energy scale in TeV when $c_i \sim 1$ (corresponding to an $\mathcal{O}(1)$ new physics coupling) and the operator normalisation is v^2/Λ^2. For $\bar{c}_W + \bar{c}_B$, whose operator normalisation is m_W^2/Λ^2, the energy scale is effectively divided by ~ 3.
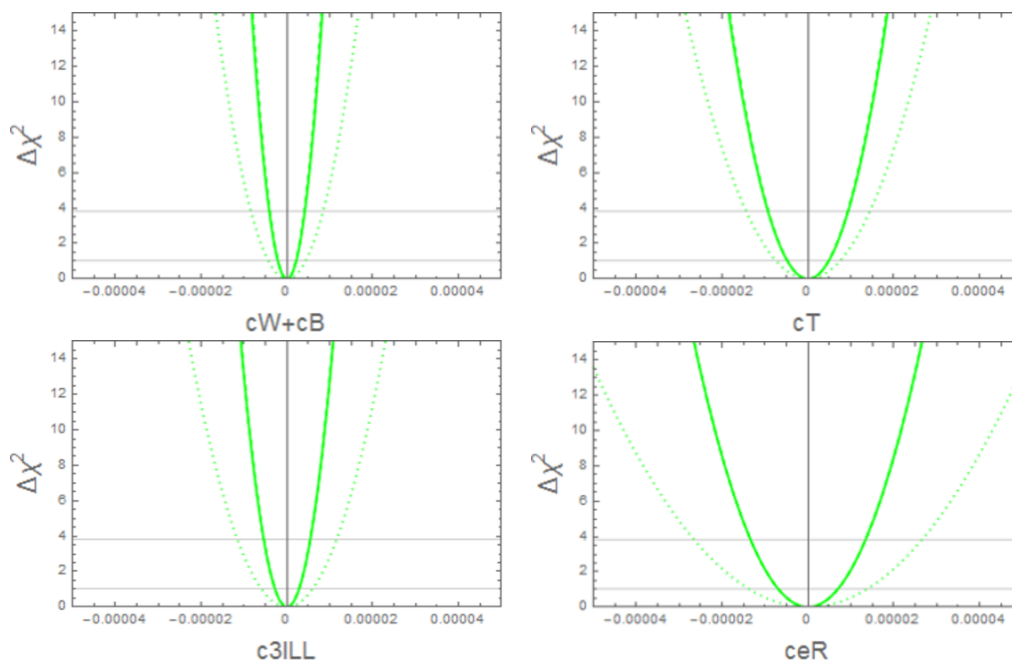
Figure 2. Prospective marginalised constraints on operator coefficients from ILC EWPT measurements. The projected $\Delta\chi^2$ for each operator affecting the leptonic subset of EWPT observables when when they are all allowed to vary simultaneously, incorporating the prospective ILC measurements [35]. The solid (dotted) lines are for dimension-6 contributions computed using the tree-level expressions with $s_W^2|^{\rm SM}$ ($s_W^2|^{\rm tree}$), whereas the dashed lines are computed numerically using `ZFITTER` in the expansion framework of [53].
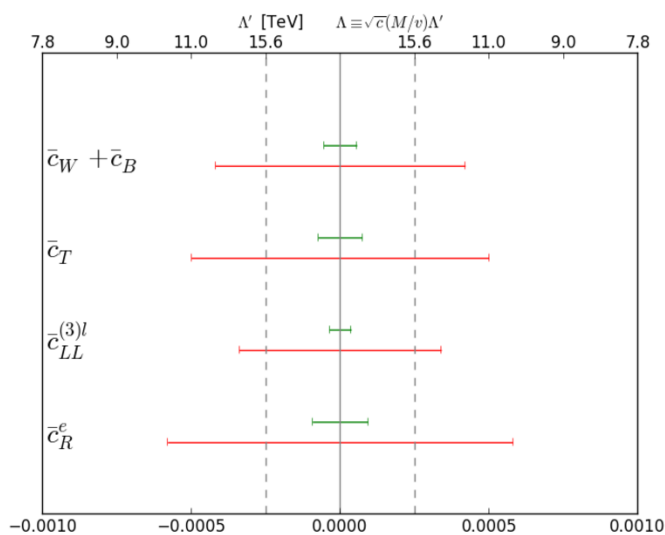
Figure 3. Summary plot of the individual (green) and marginalised (red) 95% CL limits on dimension-6 operators at ILC. The upper axis denotes the cut-off scale Λ when $c \sim 1$. For $\bar{c}_W + \bar{c}_B$ with an operator normalisation of $M^2 = m_W^2$ instead of v^2 this should be read as divided by ~ 3.

Figure 4. Prospective constraints on individual operator coefficients from FCC-ee EWPT measurements. The projected $\Delta\chi^2$ for each operator affecting the leptonic subset of EWPT observables when switched on one at a time with the others set to zero, incorporating the prospective FCC-ee measurements [40, 58]. The solid (dotted) lines are for dimension-6 contributions computed using the tree-level expressions with $s_W^2|^{\text{SM}}$ ($s_W^2|^{\text{tree}}$), whereas the dashed lines (indistinguishable here from the solid lines) are computed numerically using ZFITTER in the expansion framework of [53].
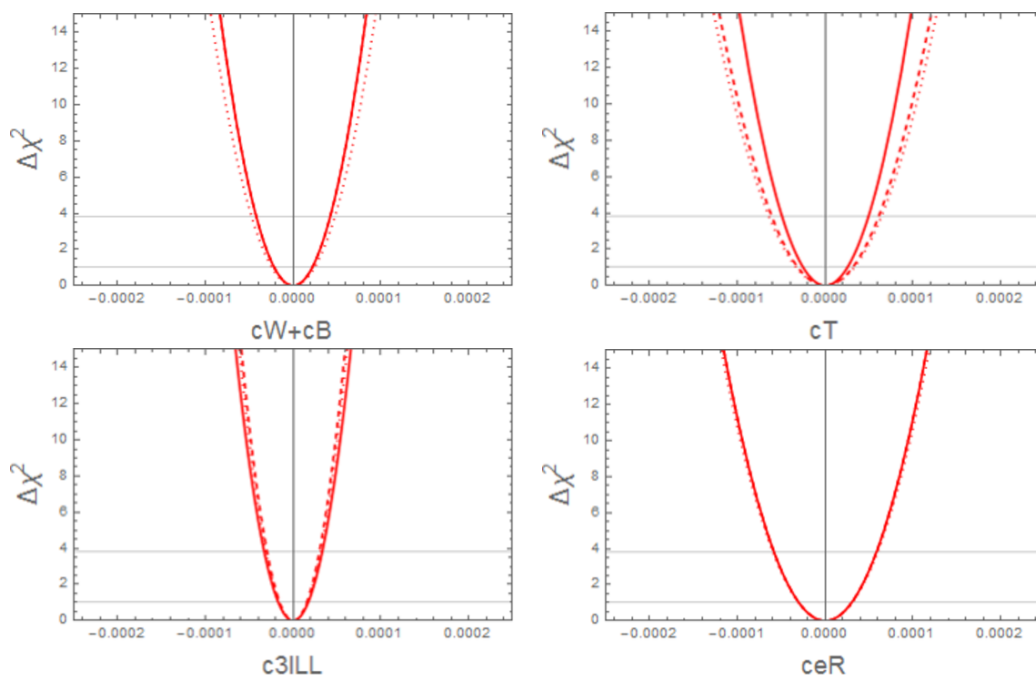
3.2 EWPT constraints from FCC-ee

We now analyse the prospective sensitivity of the FCC-ee, using the same set of four observables as for the ILC, but with the experimental errors given in [58], that are based on [40],

$$\sigma_{m_W} = 0.0005\,\text{GeV}\,, \quad \sigma_{\Gamma_Z} = 0.0001\,\text{GeV}\,, \quad \sigma_{R_l} = 0.001\,, \quad \sigma_{A_e} = 0.000015\,. \quad (3.5)$$

These errors are dominated by the systematic uncertainties, and we neglect again the theoretical uncertainties, so as to indicate the potential sensitivity of the experimental reach alone.

Figure 4 shows the χ^2 contributions from individual fits switching on the operators one at a time, and figure 5 varies them simultaneously before marginalising over the other operators. As previously, the solid and dashed lines denote the χ^2 contributions of dimension-6 operators calculated with $s_W^2|^{\text{SM}}$ using the tree-level expressions and the ZFITTER expansion coefficients of [53], respectively. They are indistinguishable in the individual fits. whereas the marginalised fit shows some small variations. The dotted lines calculated using the tree-level expressions with $s_W^2|^{\text{tree}}$ exhibit larger variations in the individual fit.

The prospective FCC-ee 95% CL constraints are summarised in dark green (red) for the individual (marginalised) limits in figure 6. Even in the marginalised case, the barred coefficients are constrained at the $\mathcal{O}(10^{-5})$ level, which translates to an indirect sensitivity in the tens of TeV, modulo the effects of weak or strong coupling in the new physics being integrated at tree or loop level.

Figure 5. Prospective marginalised constraints on operator coefficients from FCC-ee EWPT measurements. The projected $\Delta\chi^2$ is shown for each operator affecting the leptonic subset of EWPT observables when when they are all allowed to vary simultaneously, incorporating the prospective FCC-ee measurements [40, 58]. The solid (dotted) lines are for dimension-6 contributions computed using the tree-level expressions with $s_W^2|^{\rm SM}$ ($s_W^2|^{\rm tree}$), whereas the dashed lines are computed numerically using ZFITTER in the expansion framework of [53].
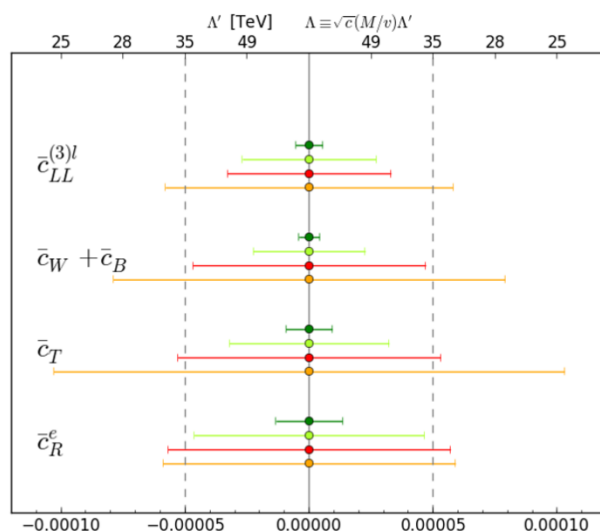
Figure 6. Projected 95% CL limits at FCC-ee$_{240\,{\rm GeV}}^{10{\rm ab}^{-1}}$ for the leptonic subset of operators affecting EWPTs. The individual (marginalised) bounds are coloured in dark green (red). The effects of theoretical uncertainties are included in light green (orange) for the individual (marginalised) fits.

– 10 –

With statistical and systematic uncertainties reduced to the levels shown in (3.5), the limiting factors in interpreting the data may well be the theoretical uncertainties that we have neglected. Attaining the optimal sensitivity to indirect effects from physics beyond the SM will require reducing these theoretical uncertainties, the effects of which can be estimated by adding in quadrature the projections from [59],

$$\sigma^{\mathrm{th}}_{\Gamma_Z} = 0.0001\,\mathrm{GeV}\,, \qquad \sigma^{\mathrm{th}}_{m_W} = 0.001\,\mathrm{GeV}\,, \qquad \sigma^{\mathrm{th}}_{A_e} = 0.000118\,.$$

The current theoretical uncertainties are $4\,\mathrm{MeV}$ for the W mass, $0.5\,\mathrm{MeV}$ for the Z decay width and 37×10^{-5} for A_l, which could be reduced to the above estimates by future three-loop level calculations [59]. The resulting individual and marginalised 95% CL constraints are shown in figure 6 in light green and orange respectively.

4 Higgs and Triple-Gauge Couplings

The Higgs production mechanism we consider for future e^+e^- colliders is associated $Z + H$ production. The dependence on the dimension-6 coefficients of the cross section for this process at a centre-of-mass energy $\sqrt{s} \sim 250\,\mathrm{GeV}$ can be expressed via a rescaling factor relative to the SM prediction that was calculated in [60], which can be translated into our basis and normalisation as

$$\frac{\delta\sigma_{\mathrm{VH}}}{\sigma_{\mathrm{VH}}} \approx 1 + 1.98\bar{c}^{(3)l}_{LL} + 1.16\bar{c}_B + 1.55\bar{c}_\gamma - 12.6\bar{c}^e_R - 0.99\bar{c}_H$$
$$- 0.77\bar{c}_{HB} + 7.74\bar{c}_{HW} - 0.661\bar{c}_T + 19.3\bar{c}_W\,,$$

where we set $\bar{c}^e_R = \bar{c}^{(3)l}_{LL} = 0$ and $\bar{c}_B = -\bar{c}_W$, due to the strong EWPT constraints on these combinations of operators described previously. The numerical dependences of the Higgs branching ratios on the dimension-6 operator coefficients are provided in [61].

For triple-gauge couplings (TGCs) we use the $e^+e^- \rightarrow W^+W^-$ cross-section rescalings at $\sqrt{s} = 200$ and $500\,\mathrm{GeV}$ calculated in [62].[7] Using the integration-by-parts identity

$$\mathcal{O}_B = \mathcal{O}_{HB} + \frac{1}{4}\mathcal{O}_{BB} + \frac{1}{4}\mathcal{O}_{WB}\,,$$

the expressions in [62] are translated into our basis and operator normalisation as

$$\left.\frac{\delta\sigma_{WW}}{\sigma_{WW}}\right|_{500\mathrm{GeV}} \approx 0.47(\bar{c}_{HW} + \bar{c}_W) + 0.52(\bar{c}_{HW} + \bar{c}_{HB}) + 0.18\bar{c}_{3W} - 0.76(\bar{c}_W + \bar{c}_B) + 22.30\bar{c}_T\,,$$
$$\left.\frac{\delta\sigma_{WW}}{\sigma_{WW}}\right|_{200\mathrm{GeV}} \approx 0.05(\bar{c}_{HW} + \bar{c}_W) + 0.095(\bar{c}_{HW} + \bar{c}_{HB}) + 0.05\bar{c}_{3W} - 0.74(\bar{c}_W + \bar{c}_B) + 14.93\bar{c}_T\,.$$

We see that the cross-section dependence on the effects of dimension-6 operators rises with the energy of diboson production, which makes this an important channel for constraining the SM EFT. As in the expressions for the Higgscouplings, we set here $\bar{c}_W + \bar{c}_B$ and $\bar{c}_T$ to zero as these are more strongly constrained by EWPTs. Since the ILC projections are given

---

[7]For other studies of dimension-6 operators in TGCs see for example refs. [31, 63–66].
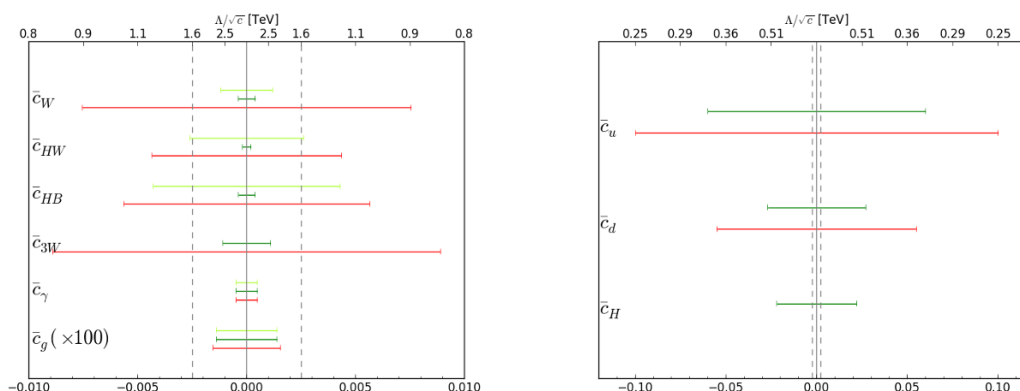
Figure 7. Summary of the 95% CL constraints on dimension-6 operator coefficients affecting Higgs and TGC observables at ILC250. The green bars indicate individual fits switching on one coefficient at a time, with light green using Higgs measurements only and dark green also including TGCs. The marginalised constraints are denoted by red bars. The upper x-axis should be rescaled by $\times 3$ ($\times 10$) for $\bar{c}_\gamma$ ($\bar{c}_g$).

only for each TGC anomalous couplings individually, and none are available for FCC-ee, we use for both ILC and FCC-ee an $\mathcal{O}(10^{-4})$ experimental sensitivity, corresponding to an improvement by two orders of magnitude over the per-cent measurements at LEP2 as estimated in ref. [39].

For examples of recent studies of current constraints on dimension-6 operators and their correlations, including the effects of differential distributions, we refer the reader to refs. [21–24, 29, 32].

4.1 Higgs and TGC constraints from the ILC

The scenario we consider is the ILC running at $250\,\text{GeV}$ with the standard luminosity of $250\ \text{fb}^{-1}$, which we call ILC250. The error projections for the different Higgs channels are taken from table 5.4 of [34], and the TGCs are included as described above. The prospective $Z\gamma$ Higgs branching ratio measurement is not reported, so we conservatively take the error on this to be 100%.

We perform a 9-parameter χ^2 fit to the operator coefficients $\{\bar{c}_W, \bar{c}_{HW}, \bar{c}_{HB}, \bar{c}_{3W}, \bar{c}_\gamma, \bar{c}_g, \bar{c}_H, \bar{c}_u$ and $\bar{c}_d\}$ using a Metropolis-Hastings algorithm. The resulting widths of the 95% CL constraints centred on zero are summarised in figure 7, and the coefficients $\bar{c}_H, \bar{c}_u, \bar{c}_d$ are shown separately with limits that are an order of magnitude worse. The dark green (red) bounds denote the individual (marginalised) fits, and we note that no meaningful constraints are placed on c_H when marginalised.

We see that even in the marginalised case the limits are at the $\sim 10^{-3}$ level, which indicates a sensitivity that begins to probe the TeV scale. This is to be contrasted with the limits on these coefficients from the LHC, which are currently at the per-cent level. The importance of including TGCs can also be seen by their effect on the individual limits when removing them from the fit, as shown in light green in figure 7. The $\bar{c}_g$ ($\bar{c}_\gamma$) coefficient
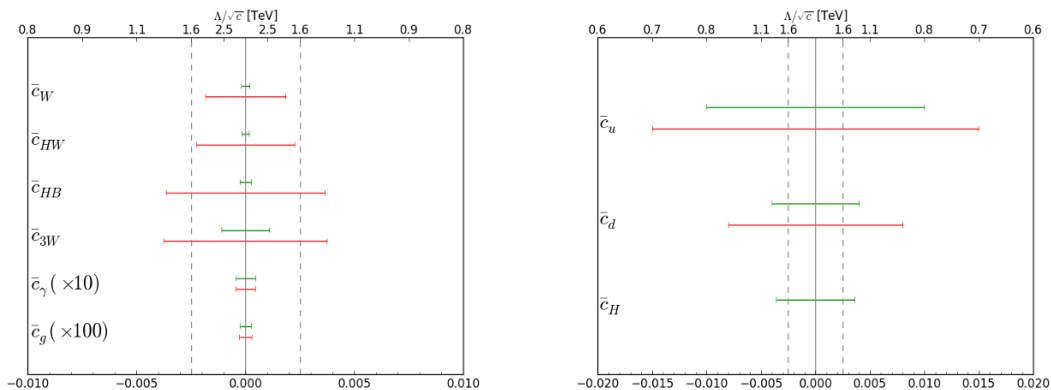
Figure 8. Summary of the 95% CL limits on dimension-6 operator coefficients affecting Higgs and TGC observables at FCC-ee. The individual (marginalised) limits are shown in green (red). The upper x-axis should be rescaled by ×3 (×10) for $\bar{c}_\gamma$ ($\bar{c}_g$).

is multiplied by 100 (10) to be visible on the same scale, which translates into multiplying the upper x-axis by $\sim$ 10 (3). The actual scales that may be indirectly probed are of course dependent on the new physics couplings and potential loop suppression factors.

4.2 Higgs and TGC constraints from FCC-ee

We consider now the FCC-ee running at 240 GeV with the standard scenario of 10 ab^{-1} of luminosity. The estimated errors for each Higgs channel are summarised in table 4 of [40], and we assume the same TGC and $Z\gamma$ Higgs branching ratio projections as for the ILC.

The results of the χ^2 fit are shown in figure 8, with the same colour codings as for the ILC250 case. We see that the 95% CL limits are now well into the TeV range. The $\bar{c}_g$ ($\bar{c}_\gamma$) coefficient is again multiplied by 100 (10) to be visible on the same scale, and we recall that the actual scales that may be indirectly probed depend on the new physics couplings and potential loop suppression factors. We see that the limits on the coefficients $\bar{c}_H, \bar{c}_u, \bar{c}_d$ are again significantly weaker than those on the other coefficients.

5 Conclusions

Until fundamentally new particles beyond the SM are discovered, the SM EFT may be viewed as the Fermi theory of the 21$^{\text{st}}$ century. It is the effective low-energy theory given all experimentally established degrees of freedom, and the objective is to measure a non-zero Wilson coefficient that might indicate the structure of new physics. The systematic classification of possible effects from decoupled new physics makes this an attractive framework for characterising the impacts of measurements across the SM as a whole.[8]

The importance of improving precision tests of the SM, in particular in the Higgs sector, strongly motivates the construction of a future lepton collider. Such proposals

---

[8]It is worth mentioning that the possible breakdown of the SM EFT assumptions in specific measurements is not a weakness, but a strength of the approach, as it could provide a consistency check that informs the way forward in investigating any new physics effects.
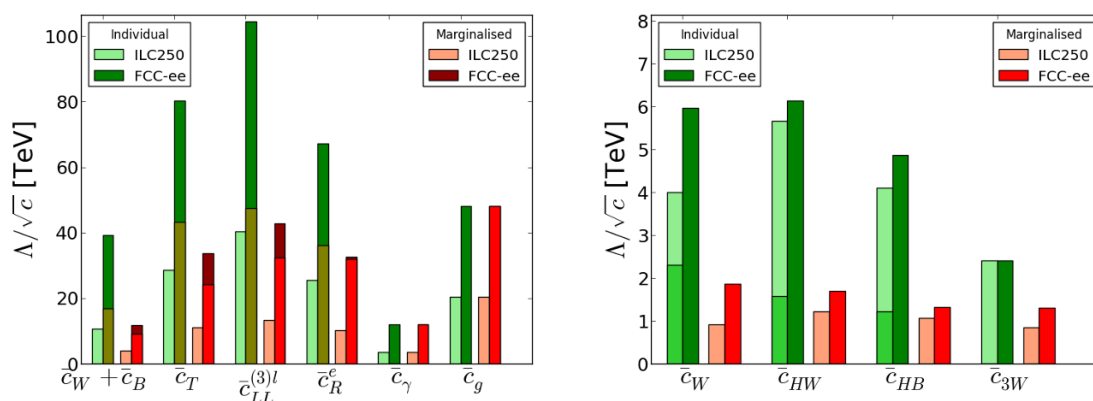
Figure 9. Summary of the reaches for the dimension-6 operator coefficients with TeV scale sensitivity, when switched on individually (green) and when marginalised (red), from projected precision measurements at the ILC250 (lighter shades) and FCC-ee (darker shades). The left plot shows the operators that are most strongly constrained by EWPTs and Higgs physics, where the different shades of dark green and dark red represent the effects of EWPT theoretical uncertainties at FCC-ee. The right plot is constrained by Higgs physics and TGCs, and the different shades of light green demonstrate the improved sensitivity when TGCs are added at ILC250.

include the ILC and FCC-ee, as well as the Chinese collider CEPC [67]. One may then ask how the improved precision of measurements at these machines translates into the scale of heavy new physics to which we shall be indirectly sensitive. The SM EFT provides a relatively model-independent way to address this question.

We have shown in this paper that the prospective sensitivities of possible future e^+e^- colliders extend to $\Lambda = \mathcal{O}(30)\,\text{TeV}$ in the case of EWPTs at FCC-ee, $\Lambda = \mathcal{O}(10)\,\text{TeV}$ in the case of EWPTs at ILC250, $\Lambda = \mathcal{O}(2)\,\text{TeV}$ in the case of Higgs and TGC measurements at FCC-ee, and $\Lambda = \mathcal{O}(1)\,\text{TeV}$ in the case of Higgs and TGC measurements at ILC250. These estimates are for the more conservative marginalised limits. The individual fits, assuming only one operator affects a given set of observables at a time, provides an upper bound on the potential reach. These results are summarised in figure 9. We expect that higher-energy runs of the ILC would improve the sensitivity to new physics via Higgs and TGC measurements, but improving its sensitivity to new physics via EWPTs would require higher luminosity at the Z peak and near the W^+W^- threshold. In this respect, the capabilities of the CEPC or the ILC with upgraded luminosity would lie between those of the ILC250 and FCC-ee.

As noted earlier in this paper, there are significant uncertainties in our analysis of EWPTs associated with the absence of a complete loop treatment of the SM EFT contributions to them. However, these uncertainties are unlikely to affect qualitatively the results of our analyses of Higgs physics and TGCs. Also as noted earlier, full exploitation of the potential of ILC and particularly FCC-ee measurements will require a new generation of precision electroweak and QCD loop calculations to match the statistical and other experimental uncertainties. These calculations, together with the inclusion of SM EFT theoretical errors, will certainly require a concerted and substantial theoretical effort.

References

[1] ATLAS collaboration, *Observation of a new particle in the search for the Standard Model Higgs boson with the ATLAS detector at the LHC*, *Phys. Lett.* **B 716** (2012) 1 [arXiv:1207.7214] [INSPIRE].

[2] CMS collaboration, *Observation of a new boson at a mass of 125 GeV with the CMS experiment at the LHC*, *Phys. Lett.* **B 716** (2012) 30 [arXiv:1207.7235] [INSPIRE].

[3] ATLAS, CMS collaborations, *Measurements of the Higgs boson production and decay rates and constraints on its couplings from a combined ATLAS and CMS analysis of the LHC pp collision data at $\sqrt{s} = 7$ and 8 TeV*, ATLAS-CONF-2015-044 (2015).

[4] T. Appelquist and J. Carazzone, *Infrared Singularities and Massive Fields*, *Phys. Rev.* **D 11** (1975) 2856 [INSPIRE].

[5] W. Buchmüller and D. Wyler, *Effective Lagrangian Analysis of New Interactions and Flavor Conservation*, *Nucl. Phys.* **B 268** (1986) 621 [INSPIRE].

[6] B. Grzadkowski, M. Iskrzynski, M. Misiak and J. Rosiek, *Dimension-Six Terms in the Standard Model Lagrangian*, *JHEP* **10** (2010) 085 [arXiv:1008.4884] [INSPIRE].

[7] S. Weinberg, *Baryon and Lepton Nonconserving Processes*, *Phys. Rev. Lett.* **43** (1979) 1566 [INSPIRE].

[8] L. Lehman, *Extending the Standard Model Effective Field Theory with the Complete Set of Dimension-7 Operators*, *Phys. Rev.* **D 90** (2014) 125023 [arXiv:1410.4193] [INSPIRE].

[9] L. Lehman and A. Martin, *Low-derivative operators of the Standard Model effective field theory via Hilbert series methods*, *JHEP* **02** (2016) 081 [arXiv:1510.00372] [INSPIRE].

[10] B. Henning, X. Lu and H. Murayama, *How to use the Standard Model effective field theory*, *JHEP* **01** (2016) 023 [arXiv:1412.1837] [INSPIRE].

[11] A. Drozd, J. Ellis, J. Quevillon and T. You, *Comparing EFT and Exact One-Loop Analyses of Non-Degenerate Stops*, *JHEP* **06** (2015) 028 [arXiv:1504.02409] [INSPIRE].

[12] A. Drozd, J. Ellis, J. Quévillon and T. You, in preparation.

[13] B. Grinstein and M.B. Wise, *Operator analysis for precision electroweak physics*, *Phys. Lett.* **B 265** (1991) 326 [ɪɴSPIRE].

[14] K. Hagiwara, S. Ishihara, R. Szalapski and D. Zeppenfeld, *Low-energy effects of new interactions in the electroweak boson sector*, *Phys. Rev.* **D 48** (1993) 2182 [ɪɴSPIRE].

[15] K. Hagiwara, R. Szalapski and D. Zeppenfeld, *Anomalous Higgs boson production and decay*, *Phys. Lett.* **B 318** (1993) 155 [hep-ph/9308347] [ɪɴSPIRE].

[16] Z. Han and W. Skiba, *Effective theory analysis of precision electroweak data*, *Phys. Rev.* **D 71** (2005) 075009 [hep-ph/0412166] [ɪɴSPIRE].

[17] T. Corbett, O.J.P. Eboli, J. Gonzalez-Fraile and M.C. Gonzalez-Garcia, *Robust Determination of the Higgs Couplings: Power to the Data*, *Phys. Rev.* **D 87** (2013) 015022 [arXiv:1211.4580] [ɪɴSPIRE].

[18] B. Dumont, S. Fichet and G. von Gersdorff, *A Bayesian view of the Higgs sector with higher dimensional operators*, *JHEP* **07** (2013) 065 [arXiv:1304.3369] [ɪɴSPIRE].

[19] M. Ciuchini, E. Franco, S. Mishima and L. Silvestrini, *Electroweak Precision Observables, New Physics and the Nature of a 126 GeV Higgs Boson*, *JHEP* **08** (2013) 106 [arXiv:1306.4644] [ɪɴSPIRE].

[20] M. Ciuchini, E. Franco, S. Mishima, M. Pierini, L. Reina and L. Silvestrini, *Update of the electroweak precision fit, interplay with Higgs-boson signal strengths and model-independent constraints on new physics*, arXiv:1410.6940 [ɪɴSPIRE].

[21] A. Pomarol and F. Riva, *Towards the Ultimate SM Fit to Close in on Higgs Physics*, *JHEP* **01** (2014) 151 [arXiv:1308.2803] [ɪɴSPIRE].

[22] J. Ellis, V. Sanz and T. You, *Complete Higgs Sector Constraints on Dimension-6 Operators*, *JHEP* **07** (2014) 036 [arXiv:1404.3667] [ɪɴSPIRE].

[23] J. Ellis, V. Sanz and T. You, *The Effective Standard Model after LHC Run I*, *JHEP* **03** (2015) 157 [arXiv:1410.7703] [ɪɴSPIRE].

[24] A. Falkowski and F. Riva, *Model-independent precision constraints on dimension-6 operators*, *JHEP* **02** (2015) 039 [arXiv:1411.0669] [ɪɴSPIRE].

[25] L. Berthier and M. Trott, *Towards consistent Electroweak Precision Data constraints in the SMEFT*, *JHEP* **05** (2015) 024 [arXiv:1502.02570] [ɪɴSPIRE].

[26] L. Berthier and M. Trott, *Consistent constraints on the Standard Model Effective Field Theory*, *JHEP* **02** (2016) 069 [arXiv:1508.05060] [ɪɴSPIRE].

[27] A. Efrati, A. Falkowski and Y. Soreq, *Electroweak constraints on flavorful effective theories*, *JHEP* **07** (2015) 018 [arXiv:1503.07872] [ɪɴSPIRE].

[28] A. Falkowski, *Effective field theory approach to LHC Higgs data*, arXiv:1505.00046 [ɪɴSPIRE].

[29] T. Corbett, O.J.P. Eboli, D. Goncalves, J. Gonzalez-Fraile, T. Plehn and M. Rauch, *The Higgs Legacy of the LHC Run I*, *JHEP* **08** (2015) 156 [arXiv:1505.05516] [ɪɴSPIRE].

[30] A. Buckley et al., *Global fit of top quark effective theory to data*, *Phys. Rev.* **D 92** (2015) 091501 [arXiv:1506.08845] [ɪɴSPIRE].

[31] A. Falkowski, M. Gonzalez-Alonso, A. Greljo and D. Marzocca, *Global constraints on anomalous triple gauge couplings in effective field theory approach*, *Phys. Rev. Lett.* **116** (2016) 011801 [arXiv:1508.00581] [ɪɴSPIRE].

[32] J. Brehmer, A. Freitas, D. Lopez-Val and T. Plehn, *Pushing Higgs Effective Theory to its Limits*, arXiv:1510.03443 [INSPIRE].

[33] A. Falkowski, B. Fuks, K. Mawatari, K. Mimasu, F. Riva and V. sanz, *Rosetta: an operator basis translator for Standard Model effective field theory*, *Eur. Phys. J.* **C 75** (2015) 583 [arXiv:1508.05895] [INSPIRE].

[34] D.M. Asner et al., *ILC Higgs White Paper*, arXiv:1310.0763 [INSPIRE].

[35] A. Freitas et al., *Exploring Quantum Physics at the ILC*, arXiv:1307.3962 [INSPIRE].

[36] T. Han, Z. Liu, Z. Qian and J. Sayre, *Improving Higgs coupling measurements through ZZ Fusion at the ILC*, *Phys. Rev.* **D 91** (2015) 113007 [arXiv:1504.01399] [INSPIRE].

[37] A. Arbey et al., *Physics at the e^+e^- Linear Collider*, *Eur. Phys. J.* **C 75** (2015) 371 [arXiv:1504.01726] [INSPIRE].

[38] K. Fujii et al., *Physics Case for the International Linear Collider*, arXiv:1506.05992 [INSPIRE].

[39] T. Barklow et al., *ILC Operating Scenarios*, arXiv:1506.07830 [INSPIRE].

[40] TLEP DESIGN STUDY WORKING GROUP collaboration, M. Bicer et al., *First Look at the Physics Case of TLEP*, *JHEP* **01** (2014) 164 [arXiv:1308.6176] [INSPIRE].

[41] M. Baak et al., *Working Group Report: Precision Study of Electroweak Interactions*, arXiv:1310.6708 [INSPIRE].

[42] J. Fan, M. Reece and L.-T. Wang, *Possible Futures of Electroweak Precision: ILC, FCC-ee and CEPC*, *JHEP* **09** (2015) 196 [arXiv:1411.1054] [INSPIRE].

[43] J. Fan, M. Reece and L.-T. Wang, *Precision Natural SUSY at CEPC, FCC-ee and ILC*, *JHEP* **08** (2015) 152 [arXiv:1412.3107] [INSPIRE].

[44] A. Thamm, R. Torre and A. Wulzer, *Future tests of Higgs compositeness: direct vs indirect*, *JHEP* **07** (2015) 100 [arXiv:1502.01701] [INSPIRE].

[45] C. Grojean, E.E. Jenkins, A.V. Manohar and M. Trott, *Renormalization Group Scaling of Higgs Operators and $\Gamma(h \to \gamma\gamma)$*, *JHEP* **04** (2013) 016 [arXiv:1301.2588] [INSPIRE].

[46] J. Elias-Miró, J.R. Espinosa, E. Masso and A. Pomarol, *Renormalization of dimension-six operators relevant for the Higgs decays $h \to \gamma\gamma, \gamma Z$*, *JHEP* **08** (2013) 033 [arXiv:1302.5661] [INSPIRE].

[47] J. Elias-Miro, J.R. Espinosa, E. Masso and A. Pomarol, *Higgs windows to new physics through $D = 6$ operators: constraints and one-loop anomalous dimensions*, *JHEP* **11** (2013) 066 [arXiv:1308.1879] [INSPIRE].

[48] E.E. Jenkins, A.V. Manohar and M. Trott, *Renormalization Group Evolution of the Standard Model Dimension Six Operators I: Formalism and lambda Dependence*, *JHEP* **10** (2013) 087 [arXiv:1308.2627] [INSPIRE].

[49] E.E. Jenkins, A.V. Manohar and M. Trott, *Renormalization Group Evolution of the Standard Model Dimension Six Operators II: Yukawa Dependence*, *JHEP* **01** (2014) 035 [arXiv:1310.4838] [INSPIRE].

[50] R. Alonso, E.E. Jenkins, A.V. Manohar and M. Trott, *Renormalization Group Evolution of the Standard Model Dimension Six Operators III: Gauge Coupling Dependence and Phenomenology*, *JHEP* **04** (2014) 159 [arXiv:1312.2014] [INSPIRE].

[51] J. Elias-Miró, C. Grojean, R.S. Gupta and D. Marzocca, *Scaling and tuning of EW and Higgs observables*, *JHEP* **05** (2014) 019 [arXiv:1312.2928] [INSPIRE].

[52] R. Alonso, H.-M. Chang, E.E. Jenkins, A.V. Manohar and B. Shotwell, *Renormalization group evolution of dimension-six baryon number violating operators*, *Phys. Lett.* **B 734** (2014) 302 [arXiv:1405.0486] [INSPIRE].

[53] J.D. Wells and Z. Zhang, *Precision Electroweak Analysis after the Higgs Boson Discovery*, *Phys. Rev.* **D 90** (2014) 033006 [arXiv:1406.6070] [INSPIRE].

[54] D.Yu. Bardin et al., *ZFITTER v.6.21: A semianalytical program for fermion pair production in e^+e^- annihilation*, *Comput. Phys. Commun.* **133** (2001) 229 [hep-ph/9908433] [INSPIRE].

[55] M. Ghezzi, R. Gomez-Ambrosio, G. Passarino and S. Uccirati, *NLO Higgs effective field theory and κ-framework*, *JHEP* **07** (2015) 175 [arXiv:1505.03706] [INSPIRE].

[56] C. Hartmann and M. Trott, *Higgs Decay to Two Photons at One Loop in the Standard Model Effective Field Theory*, *Phys. Rev. Lett.* **115** (2015) 191801 [arXiv:1507.03568] [INSPIRE].

[57] A. David and G. Passarino, *Through precision straits to next standard model heights*, *Rev. Phys.* **1** (2016) 13 [arXiv:1510.00414] [INSPIRE].

[58] A. Blondel, *Exploring the Physics Frontier with Circular Colliders*, Aspen, Colorado, U.S.A., 31 January 2015: http://http://indico.cern.ch/event/336571/.

[59] S. Mishima, *Sensitivity to new physics from TLEP precision measurements*, *6th TLEP workshop*, CERN, 16 October 2013: http://indico.cern.ch/event/257713/session/1/contribution/30.

[60] N. Craig, M. Farina, M. McCullough and M. Perelstein, *Precision Higgsstrahlung as a Probe of New Physics*, *JHEP* **03** (2015) 146 [arXiv:1411.0676] [INSPIRE].

[61] R. Contino, M. Ghezzi, C. Grojean, M. Mühlleitner and M. Spira, *eHDECAY: an Implementation of the Higgs Effective Lagrangian into HDECAY*, *Comput. Phys. Commun.* **185** (2014) 3412 [arXiv:1403.3381] [INSPIRE].

[62] J.D. Wells and Z. Zhang, *Status and prospects of precision analyses with $e^+e^- \to W^+W^-$*, *Phys. Rev.* **D 93** (2016) 034001 [arXiv:1507.01594] [INSPIRE].

[63] L. Bian, J. Shu and Y. Zhang, *Prospects for Triple Gauge Coupling Measurements at Future Lepton Colliders and the 14 TeV LHC*, *JHEP* **09** (2015) 206 [arXiv:1507.02238] [INSPIRE].

[64] B. Gripaios and D. Sutherland, *Searches for CP-violating dimension-6 electroweak gauge boson operators*, *Phys. Rev.* **D 89** (2014) 076004 [arXiv:1309.7822] [INSPIRE].

[65] T. Corbett, O.J.P. É boli, J. Gonzalez-Fraile and M.C. Gonzalez-Garcia, *Determining Triple Gauge Boson Couplings from Higgs Data*, *Phys. Rev. Lett.* **111** (2013) 011801 [arXiv:1304.1151] [INSPIRE].

[66] C. Bobeth and U. Haisch, *Anomalous triple gauge couplings from B-meson and kaon observables*, *JHEP* **09** (2015) 018 [arXiv:1503.04829] [INSPIRE].

[67] CEPC-SPPC Study Group, *CEPC-SPPC Preliminary Conceptual Design Report. 1. Physics and Detector*, IHEP-CEPC-DR-2015-01, IHEP-TH-2015-01, HEP-EP-2015-01 [INSPIRE].